Mathematical puzzle based PV array configuration for GMP enhancement under non-uniform irradiation

Isha Kansal[1], Rupendra Pachauri[1,*]

[1]Department of Electrical and Electronics Engineering, School of Engineering, University of Petroleum and Energy Studies, Dehradun, India- 248007

Abstract

The performance exploration of the proposed PV array configurations is analysed during the shadowing conditions. The performance evaluation of total-cross-tied (TCT) and symmetric matrix-total-cross-tied (SM-TCT) pattern based electrical connections are assessed according to distinguish shadow test cases. The PV system's non-linear conduct is noted in terms of I-V and P-V curves. During partial shading conditions (PSCs), multiple power points (MPP) are observed such as local MPP and global MPP. Both TCT and SM-TCT configurations are compared in terms of parameters Global MPP, fill factor (FF) and performance enhancement (PE) under the three distinct shadow test cases as (i) lamp post (ii) three cornered shading or structure shadow (iii) single vertex shading respectively.

1. Introduction

Because of the depletion of fossil fuels and environmental pollution concerns, renewable energy (RE) based generation research is rapidly growing up today [1]. Due to numerous benefits, the electrical power consumed is rising rapidly. At present, the PV system is at most capable source of RE. Because of its wide advantages features such as, no adverse effect on environmental and less maintenance requirements, the PV system has wide acceptability [2]. It is a big challenge to improve the electrical power rating from the PV array system under shaded conditions (Partially or fully). In this context, many methods for achieving the maximum power are reported in the existing literature. The shadowing condition has a big role in diminishing the PV array performance. In addition of this, the basic causes of PSCs are trees shadow, buildings, cloud positions. Moreover, due to hotspot conditions, the PV cells are damaged. In anti-parallel with PV cells the same issue uses bypass diodes [3, 4] and this problem can be addressed easily.

1.1. Literature review

Currently, various researchers are exploring various solutions to enhance the performance of PV systems by using satisfactory methods such as bypass diode integration with modules and altering the position of the PV module with fixed electrical connections in a range. One of the most appropriate methods available in the current scenario is to reconfigure PV modules in PV array schemes is reported in the recent literature available. The PV modules are generally arranged electrically as series and/or parallel for load power requirement. When one or more solar panels are shaded, the generation of power from the PV array decreases considerably. In [5], the writers rearranged in a PV matrix the traditional total cross-tied (TCT) links of embedded components centred on Su-Do-Ku puzzle. In addition, comprehensive research is carried out to compare the outcomes acquired such as energy failures, FF and GMPP location of both settings under the four kinds of shading instances such as short narrow (SN), short wide (SW), long narrow (LN) and long wide (LW). In an experimental research, local and GMPPs are recognized and validated under shading circumstances with the MATLAB/Simulink

*Corresponding author. Email: rpachauri@ddn.upes.ac.in

model [6]. Connected series three screens are regarded to determine the effect of un-even irradiance at the GMPP location [7]. In order to achieve the MPPT during the shaded series-parallel (SP), TCT and bridge-link (BL) arranged PV modules, an experimental and MATLAB/Simulink study is conducted. The highest outcomes relative to other modules are determined by TCT [8, 9]. The writers of [10, 11] intended the 3 range size of PV array in sequence links to demonstrate the shadowing effect on the P-V curve and the GMPP is 40W. In [12] under three shading circumstances, an inquiry is carried out into the sequence and simultaneous relations of the PV grid. The outcomes for enhanced FF, small mismatch losses (MML) and a minimum amount of GMPPs for parallel links are noted. For the testing of 230W PV panels (eight digits) organized in sequence links and conducted under three shading test systems, simulated and experimental outcomes are contrasted. The placement of bypass diode with the PV cell cords is evaluated during the research to reduce the shadowing effect [13]. The technique of optimization is used to disperse the shadow on the TCT connections of the PV panel and thus contrasted the outcomes with Su-Do-Ku puzzle-based links in terms of energy improvement, enhanced FF and minimal energy losses under PSCs [14]. For comprehensive research under PSCs, PV array settings such as sequence, parallel, TCT, bridge-link (BL), honey-comb (HC) and fresh PV array setup are studied in [15]. Compared to others, the proposed ' NEW' configuration has best results. An enhanced Su-Do-Ku model is obtained from Su-Do-Ku electrical connections given in [16] for exploring efficiency in four shadow experiments: short wide (SW), long wide (LW), short narrow (SN) and long narrow (LN).In addition, Su-Do-Ku has the highest outcomes in all the enhanced experiment instances as minimal energy losses are observed [17]. In [18], for SP, HC, BL, TCT and Su-Do-Ku settings, writers regarded crossing clouds as a shadow impact on the PV panel. The normal TCT and Su-Do-Ku puzzle-based TCT (RTCT) PV array set-up performance is compared with the specific shadow motifs [19]. Results from TCT, hybrid SP-TCT and Su-Do-Ku settings are analysed and discovered that PV array Su-Do-Ku links have stronger findings in terms of elevated FF, reduced power loss and fewer MPPs (P-V curve smoothness) [20]. Under SW, LW, SN and LN shading circumstances, the production strength of a PV system increases by using various settings such as electrical panel setup (EAR), Futoshiki, and module-fixed electrical link (PRM-FEC) physical transfer [20, 21]. Optimum PV panel links in an array are chosen and contrasted under the predefined shading impacts with standard SP and TCT panel interconnections and discovered that optimum links have highest results [22]. Authors developed an electromechanical relay-based hardware system to switch 3x3 complete TCT connections from SP configuration [23]. PV system output analysis is performed efficiently at global maximum power point (GMPP), power loss, and FF in terms of power and voltage. Simulation MATLAB validates all hardware tests. MATLAB simulation validates all hardware results. A thorough fault analysis including non-uniform shading on SP, HC, and TCT PV systems is presented. A special case of non-uniform irradiance multiple PV array faults is also investigated to examine their cumulative effect on different PV interconnections [24].

2. PV system and proposed configuration

2.1. Solar PV system

The electrical-equivalent circuit illustrated in Figure 1 of solar cell is capable of transforming sunlight into dc present and PV impact voltage as,
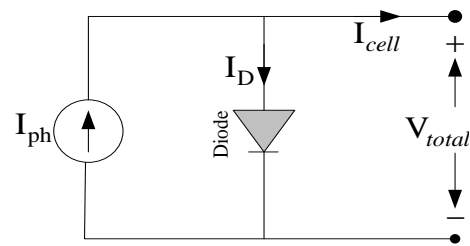

Figure 1. Solar cell electrical circuit

Deliberated current of solar cell (I_{cell}) can be articulated in equations as,

$$I_{cell} = I_{ph} - I_D \tag{1}$$

$$I_{cell} = I_{ph} - I_o \left(\exp^{\left(\frac{qV_C}{AkT_C} \right)} - 1 \right) \tag{2}$$

Where, I_{ph}: Solar Cell's photocurrent (A), I_D: diode's current (A), I_o: diode current (reverse saturation) (A), q: electron charge (Coulomb), V_C: cell voltage (V), A: ideality factor, k: Constant (Boltzmann's) (J/K) and T_C: cell temp. (°C).

2.2. SM-TCT PV array configuration

In this paper, The SM-based electrical connections for the relative study of pre-existing TCT connection in three different dynamic shading cases. SM is a technique of positioning of figures dependent on logic and these figures are unique because the summation of all figures in row or column outcomes is the same amount. In addition, with the same amount, each diagonal digit is reiterated itself. The fundamental characteristics of a SM setup of 8x8 size are displayed in Figure 2(a)-(e) as,

1	2	3	4	5	6	7	8
2	3	4	5	6	7	8	1
3	4	5	6	7	8	1	2
4	5	6	7	8	1	2	3
5	6	7	8	1	2	3	4
6	7	8	1	2	3	4	5
7	8	1	2	3	4	5	6
8	1	2	3	4	5	6	7

(a) Row-wise summation

1	2	3	4	5	6	7	8
2	3	4	5	6	7	8	1
3	4	5	6	7	8	1	2
4	5	6	7	8	1	2	3
5	6	7	8	1	2	3	4
6	7	8	1	2	3	4	5
7	8	1	2	3	4	5	6
8	1	2	3	4	5	6	7

(b) Column- wise summation

1	2	3	4	5	6	7	8
2	3	4	5	6	7	8	1
3	4	5	6	7	8	1	2
4	5	6	7	8	1	2	3
5	6	7	8	1	2	3	4
6	7	8	1	2	3	4	5
7	8	1	2	3	4	5	6
8	1	2	3	4	5	6	7

(c) Repeated one diagonal digits

	C₁	C₂	C₃	C₄	C₅	C₆	C₇	C₈
R₁	1	2	3	4	5	6	7	8
R₂	2	3	4	5	6	7	8	1
R₃	3	4	5	6	7	8	1	2
R₄	4	5	6	7	8	1	2	3
R₅	5	6	7	8	1	2	3	4
R₆	6	7	8	1	2	3	4	5
R₇	7	8	1	2	3	4	5	6
R₈	8	1	2	3	4	5	6	7

(d) Repeated SM sub-matrix

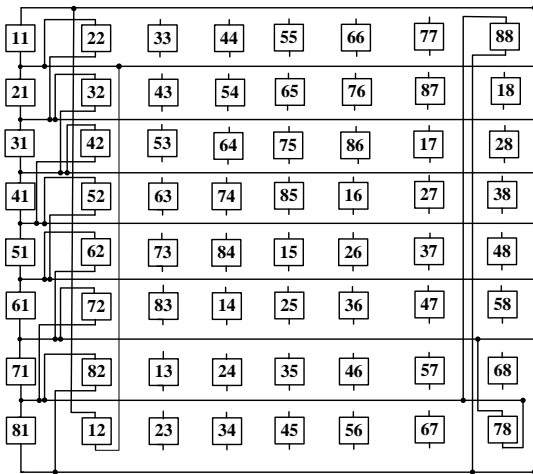|	C₁	C₂	C₃	C₄	C₅	C₆	C₇	C₈
R₁	11	22	33	44	55	66	77	88
R₂	21	32	43	54	65	76	87	18
R₃	31	42	53	64	75	86	17	28
R₄	41	52	63	74	85	16	27	38
R₅	51	62	73	84	15	26	37	48
R₆	61	72	83	14	25	36	47	58
R₇	71	82	13	24	35	46	57	68
R₈	81	12	23	34	45	56	67	78

(e) SM-TCT configuration

Figure 2(a)-(e) Symmetric matrix: Properties

As illustrated in Figure 2(a)-(e), the arithmetic addition of each row-column is shown to be 36. In addition, as shown in Fig. 2(d), the recurrence of opposite 4x4 size matrix elements exists. Moreover, there is a repeat of inverse 4x4 size matrix components as shown in Fig. 2(d). Accordingly, the characteristics are validated for 8x8 size SM. The row amount and column length of the 8x8 size PV array is depicted by the first and second digits accordingly.

The methodology for reconfiguring TCT in SM-TCT connections is shown in Figure 3(a)-(b). The proposed configuration reallocates the shadowing effect through dispersion over the modules in an array and shows momentous reduction in shading area of PV modules in different rows and columns, leading to enhancement in the system performance. It's obvious from Figure 3(b) the 22-number PV module (2nd row and 2nd column) is physically situated in the first and successive second rows in place of second row-column. So, similar methodology is executed for the entire PV panels in an array system.

11	12	13	14	15	16	17	18
21	22	23	24	25	26	27	28
31	32	33	34	35	36	37	38
41	42	43	44	45	46	47	48
51	52	53	54	55	56	57	58
61	62	63	64	65	66	67	68
71	72	73	74	75	76	77	78
81	82	83	84	85	86	87	88
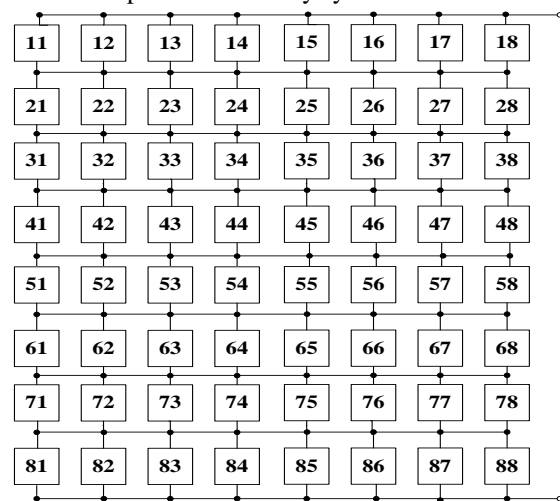
(a) TCT configuration

(b) SM-TCT configuration

Figure 3(a)-(b) TCT and SM-TCT electrical interconnections

2.3. Rules of 8x8 size SM-TCT configuration

The pth row and q^{th} column of a pattern for n^{th} element corresponding, n_{pq} is written as,

$$n_{pq}, where \begin{cases} p = no.\ of\ row & (p = 1\ to\ 8) \\ q = no.\ of\ column & (q = 1\ to\ 8) \end{cases}$$

(i) Row, column and diagonal wise summation/ analysis
Row, column and diagonal wise summation/analysis for 8x8 size SM matrix are depicted in Fig. 3(a)-(c) is expressed in Eq. (3)-(5).

$$\sum_{p=1}^{8} n_{pq} = Aggregate\ for\ p^{th} row,\quad (p = 1\ to\ 8) \tag{3}$$

$$\sum_{q=1}^{8} n_{pq} = Aggregate\ for\ q^{th} column,\quad (q = 1\ to\ 8) \tag{4}$$

$$R_n C_{m-7} = R_{n-1} C_{m-6} = ... R_{n-7} C_m \quad (where,\ n,m=8) \tag{5}$$

3. Shading cases and performance analysis

For this extensive investigation, PSCs (cases: I-III) are considered more appropriate and likely to occur for both PV modules electrical connections.

3.1. Regular shading shapes

For extensive investigation, regular partial shading forms are considered such as (i) lamp post (ii) three corner shape (iii) single vertex shading shape as depicted in Figure 4(a)-(c).

(a) Case- I: Street light shape shading

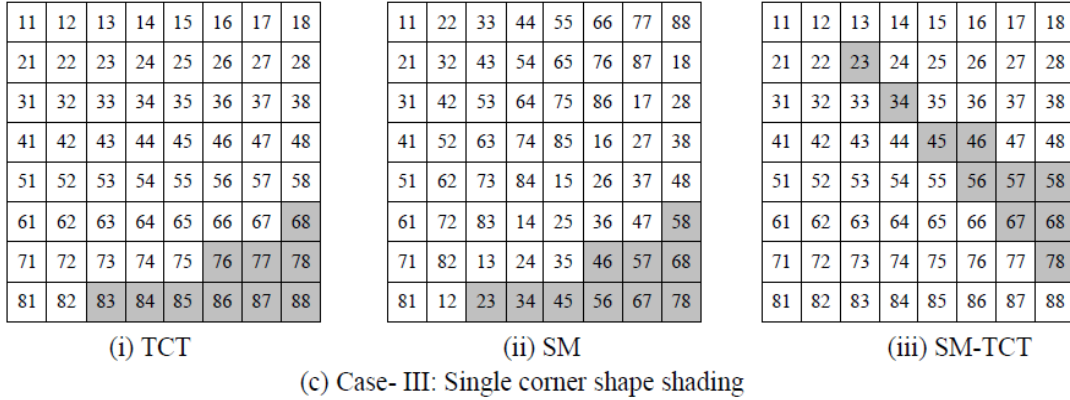(b) Case- II: Triangular or building shape shading

Fig. 4(a)-(c) Special regular shading cases for performance investigation on PV array of size 8×8

3.2. Partial shading losses

Due to partial shading, the grid energy is distinct from the energy produced at MPPT from the person PV unit, resulting in energy failures. When the PV system is partially obscured, diode is avoided, resulting in the MPP monitoring scheme being misled into operating at the LMPP as a GMPP replacement. The obtained power losses (PL) are expressed as,

$$PL = MP \text{ (without shading)} - \text{Global MP (under shading)} \quad (6)$$

3.3. Fill factor

The FF is GMPP's energy proportion to the open circuit voltage item and PV cell's brief circuit current. In addition, FF values are calculated using the I-V characteristics using Eq. (7) as,

$$\text{Fill factor} = \frac{\text{Global Maximum Power}}{\left(V_{o.c.}\right)\left(I_{s.c.}\right)} \quad (7)$$

4. Results and discussion

For the extensive performance comparison between the both PV arrays connections under three diverse shading test cases: I- III are taken. In Eq. (6), PV array voltage can be articulated,

$$Array\ Voltage = \sum_{i=1}^{i=8} V_{N_i} \quad (8)$$

Where, V_{ni} expresses the array voltage of ith row. Furthermore, the obtained row current of TCT configuration can be obtained by using Eqns. (9)-(13) under the shading case- I as,

$$I_{R1} = I_{R2} = I_{R3} = I_N + I_N + I_N + I_N + I_N + I_N + I_N + I_N = 8 \times I_N \quad (9)$$

$$I_{R4} = I_N + I_N + 0.5 \times I_N + 0.5 \times I_N + 0.5 \times I_N + I_N + I_N + I_N = 6.5 \times I_N \quad (10)$$

$$I_{R5} = 0.5 \times I_N + 0.5 \times I_N + 0.5 \times I_N + 0.5 \times I_N + 0.5 \times I_N + I_N + I_N + I_N = 5.5 \times I_N \quad (11)$$

$$I_{R6} = I_N + I_N + 0.5 \times I_N + 0.5 \times I_N + 0.5 \times I_N + I_N + I_N + I_N = 6.5 \times I_N \quad (12)$$

$$I_{R7} = I_{R8} = I_N + I_N + I_N + I_N + I_N + I_N + I_N + I_N = 8 \times I_N \quad (13)$$

Therefore, due to the shading effect, the values of generated currents in different rows are found unequal. The P-V curves display more than one power points such as Local and global MPP. Due to the voltage drop in the bypass diode, small variation of voltage in row can be ignored and voltage of PV array is calculated by using Eq. (14). If no row is circumvented and entire PV modules receive the equal irradiance.

$$P_{array} = V_{array} \times 8I_N \quad (14)$$

The current is calculated and expressed in Eqns. (15)-(21) in each row of SM-TCT PV array system for PSCs.

$$I_{R1} = I_N + I_N + I_N + 0.5 \times I_N + 0.5 \times I_N + I_N + I_N + I_N = 7 \times I_N \quad (15)$$

$$I_{R2} = I_N + I_N + I_N + I_N + 0.5 \times I_N + I_N + I_N + I_N = 7.5 \times I_N \quad (16)$$

$$I_{R3} = I_{R4} = I_N + I_N + I_N + I_N + I_N + I_N + I_N + I_N = 8 \times I_N \quad (17)$$

$$I_{R5} = 0.5 \times I_N + I_N + I_N + I_N + I_N + I_N + I_N + I_N = 7.5 \times I_N \quad (18)$$

$$I_{R6} = I_N + 0.5 \times I_N + 0.5 \times I_N + I_N + I_N + I_N + I_N + I_N = 7 \times I_N \qquad (19)$$

$$I_{R7} = I_N + I_N + 0.5 \times I_N + 0.5 \times I_N + I_N + I_N + I_N + I_N = 7 \times I_N \qquad (20)$$

$$I_{R8} = I_N + I_N + 0.5 \times I_N + 0.5 \times I_N + 0.5 \times I_N + I_N + I_N + I_N = 6.5 \times I_N \qquad (21)$$

The present results acquired in each line in the SM-TCT system are different and have the same GMPPs. Similar outcomes with regard to the resulting line current, voltage and energy are shown in Tables 1 and 2 for all deemed shading instances. Power enhancement is validated for SM-TCT scheme in all the shading cases discussed. In all the shading instances mentioned, power enhancement is validated for the SM-TCT system.

4.1. P-V and I-V curves for considered configurations

In special regular PSCs: I-III, the P-V curves of 8x8 sized TCT and SM-TCT were obtained, are shown in Fig. 5(a)-(c). GMP for traditional TCT array design is 8163W in a single regular case-I shading. In addition, the GMP acquired in the SM-TCT panel setup is greater than 9141W. Fig. 5(a) shows the P-V curves for conventional TCT and suggested SM-TCT settings for periodic shading case-I. It has been noted that the SM-TCT setup minimizes the likelihood of monitoring the incorrect MPPT and produces full energy. In all regular shading cases, the GMP array for the proposed SM-TCT scheme increased compared to conventional TCT configurations.
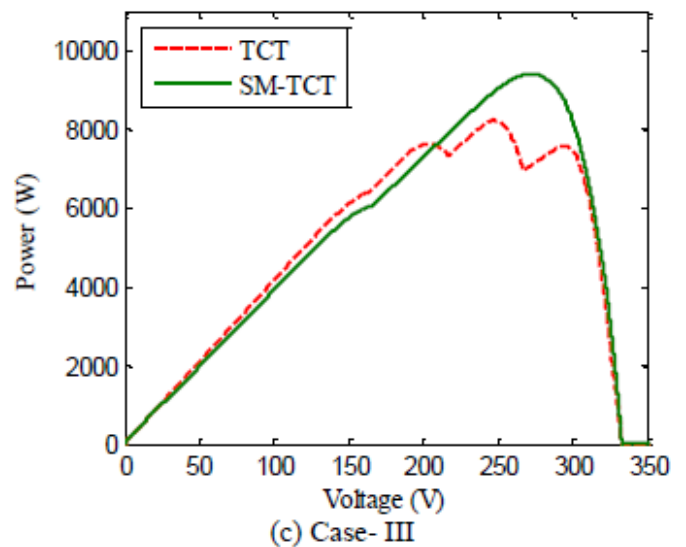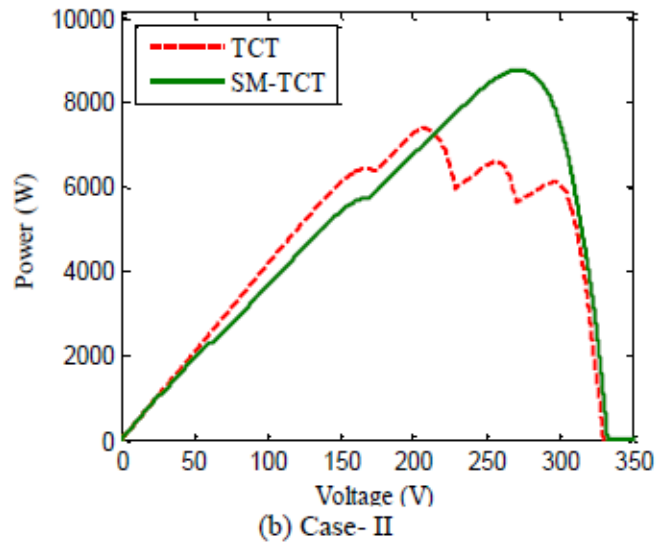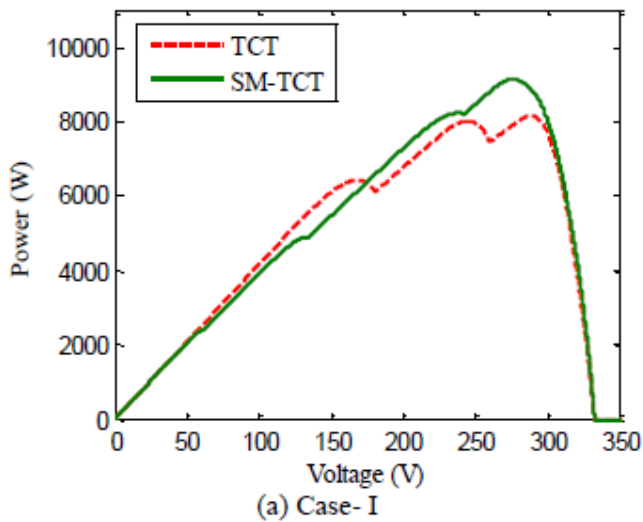

(b) Case- II

(c) Case- III

(a) Case- I

Figure 5(a)-(c). P–V curves for regular shading test cases: I- III

Table-1. Theoretical analysis of row wise voltage, current and power of PV array under shadow test cases

Partial Shading Cases	TCT			SM-TCT		
	Row current (with by passed PV modules)	Array Voltages	Array Power	Row current (with by passed PV modules)	Array Voltages	Array Power
Case-I	I_{R8} $8I_N$	$8V_N$	$64I_NV_N$	I_{R8} $6.5I_N$	$8V_N$	$52I_NV_N$
	I_{R7} $8I_N$	$7V_N$	$56I_NV_N$	I_{R7} $7I_N$	$7V_N$	$49I_NV_N$
	I_{R6} $6.5I_N$	$6V_N$	$39I_NV_N$	I_{R6} $7I_N$	$6V_N$	$42I_NV_N$
	I_{R5} $5.5I_N$	$5V_N$	$27.5I_NV_N$	I_{R5} $7.5I_N$	$5V_N$	$37.5I_NV_N$
	I_{R4} $6.5I_N$	$4V_N$	$26I_NV_N$	I_{R4} $8I_N$	$4V_N$	$32I_NV_N$
	I_{R3} $8I_N$	$3V_N$	$24I_NV_N$	I_{R3} $8I_N$	$3V_N$	$24I_NV_N$
	I_{R2} $8I_N$	$2V_N$	$16I_NV_N$	I_{R2} $7.5I_N$	$2V_N$	$15I_NV_N$
	I_{R1} $8I_N$	V_N	$8I_NV_N$	I_{R1} $7I_N$	V_N	$7I_NV_N$
Case-II	I_{R8} $4I_N$	$8V_N$	$32I_NV_N$	I_{R8} $7I_N$	$8V_N$	$56I_NV_N$
	I_{R7} $5I_N$	$7V_N$	$35I_NV_N$	I_{R7} $7.5I_N$	$7V_N$	$52.5I_NV_N$
	I_{R6} $7I_N$	$6V_N$	$42I_NV_N$	I_{R6} $7.5I_N$	$6V_N$	$45I_NV_N$
	I_{R5} $8I_N$	$5V_N$	$40I_NV_N$	I_{R5} $7I_N$	$5V_N$	$35I_NV_N$
	I_{R4} $8I_N$	$4V_N$	$32I_NV_N$	I_{R4} $7I_N$	$4V_N$	$28I_NV_N$
	I_{R3} $8I_N$	$3V_N$	$24I_NV_N$	I_{R3} $7I_N$	$3V_N$	$21I_NV_N$
	I_{R2} $8I_N$	$2V_N$	$26I_NV_N$	I_{R2} $6.5I_N$	$2V_N$	$13I_NV_N$
	I_{R1} $8I_N$	V_N	$8I_NV_N$	I_{R1} $6.5I_N$	V_N	$6.5I_NV_N$
Case-III	I_{R8} $5I_N$	$8V_N$	$40I_NV_N$	I_{R8} $8I_N$	$8V_N$	$64I_NV_N$
	I_{R7} $6.5I_N$	$7V_N$	$45.5I_NV_N$	I_{R7} $7.5I_N$	$7V_N$	$52.5I_NV_N$
	I_{R6} $7.5I_N$	$6V_N$	$45I_NV_N$	I_{R6} $7I_N$	$6V_N$	$42I_NV_N$
	I_{R5} $8I_N$	$5V_N$	$40I_NV_N$	I_{R5} $6.5I_N$	$5V_N$	$32.5I_NV_N$
	I_{R4} $8I_N$	$4V_N$	$32I_NV_N$	I_{R4} $7I_N$	$4V_N$	$28I_NV_N$
	I_{R3} $8I_N$	$3V_N$	$24I_NV_N$	I_{R3} $7.5I_N$	$3V_N$	$22.5I_NV_N$
	I_{R2} $8I_N$	$2V_N$	$26I_NV_N$	I_{R2} $7.5I_N$	$2V_N$	$15I_NV_N$
	I_{R1} $8I_N$	V_N	$8I_NV_N$	I_{R1} $8I_N$	V_N	$8I_NV_N$

In consider regular shading cases: I-III, Fig. 6(a)-(c) depicts the performance conduct of the standard TCT I V curves and the suggested fresh SM-TCT PV array settings. The electrical response is found smoother than the conventional TCT configuration.
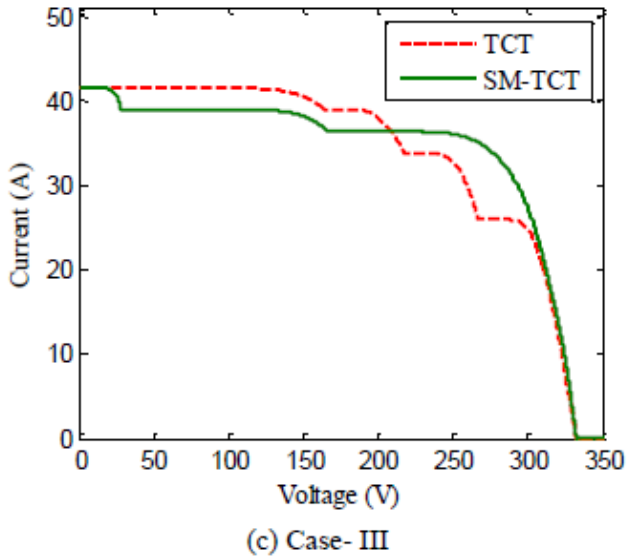

(a) Case- I

(b) Case- II
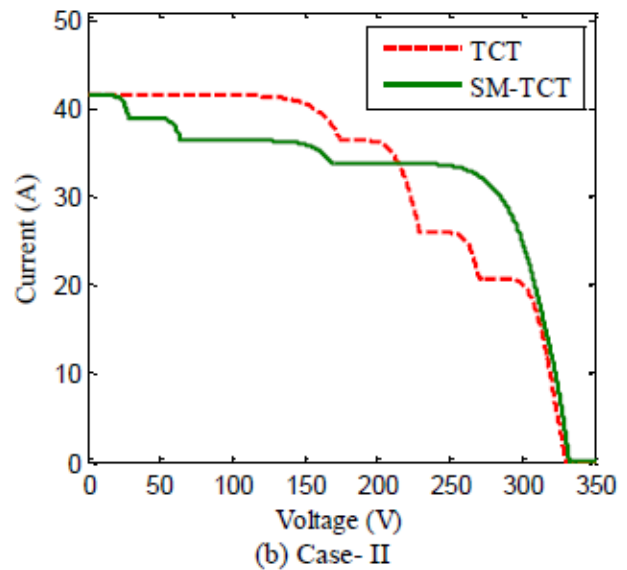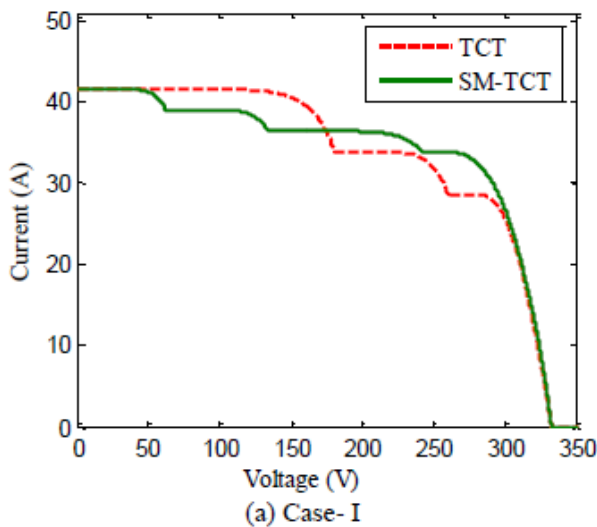
Figure 6(a)-(c) Obtained I–V curves for the shading cases: I- III

4.2. Power loss

The power at GMPP is acquired as 10440W for without shading effect and the evaluated losses (percentage) for the TCT and SM-TCT connections are summarized in Table 2. In addition, an extensive comparison of the obtained results are presented in Figure 7.

4.3. Mismatch power loss

The sum of the raised PV system individual peak power values are 0.8283kW, 1.2048kW and 0.753kW as observed.

The estimated proportion for losses in both settings is shown in Table 2 and contrasted with bar chart in Fig. 8 as,
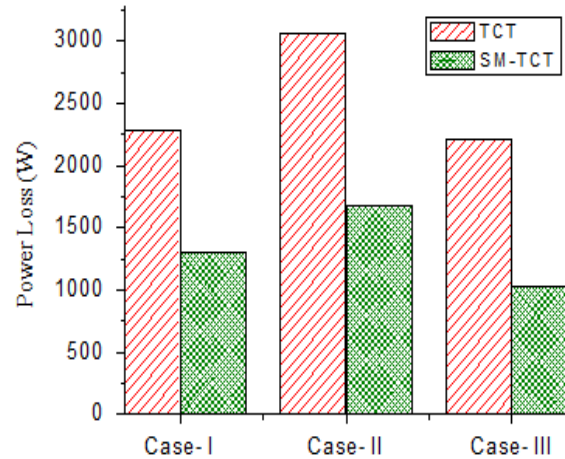

Fig. 7 Power loss for regular shading cases: I-III in TCT and SM-TCT configurations
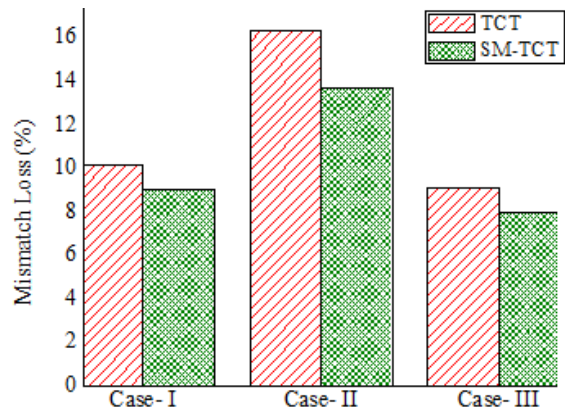

Fig. 8 Mismatch loss for regular shading cases: I-III in TCT and SM-TCT configurations

Table 2. Performance parameters f proposed investigation

Estimated Performance parameters	Case-I		Case-II		Case-III	
	TCT	SM-TCT	TCT	SM-TCT	TCT	SM-TCT
Power at GMPP (kW)	8.163	9.141	7.382	8.769	8.226	9.415
Voltage at GMPP (kV)	0.289	0.276	.2072	0.2715	0.2465	0.2726
V_{OC} (V)	332.5	332.5	329.6	332.2	332	332
I_{SC} (A)	41.5	41.5	41.6	41.6	41.5	41.5
Power losses (kW)	2.277	1.299	3.058	1.671	2.214	1.025
MML (%)	10.14	9.06	16.32	13.73	9.15	7.99
FF (%)	0.59	0.661	0.538	0.634	0.595	0.681
PR	0.781	0.875	0.707	0.839	0.787	0.901
PE(%)	_--	10.69	--	15.81	--	12.62

4.4. Power enhancement (PE) and FF

The performance parameters of PE and FF are assessed under the considered shadowing cases, which are compared using the bar chart in Figure 9 and 10 as,
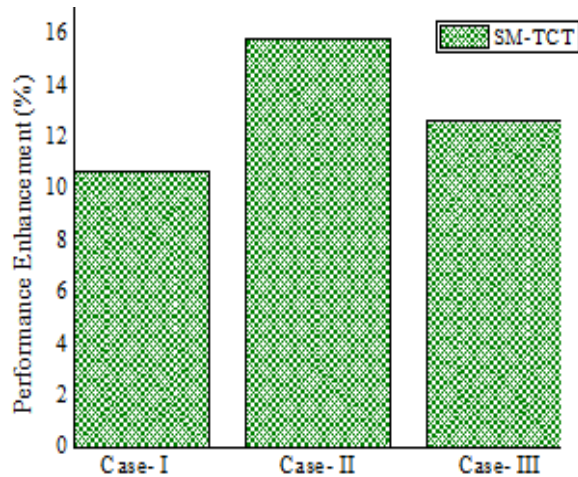
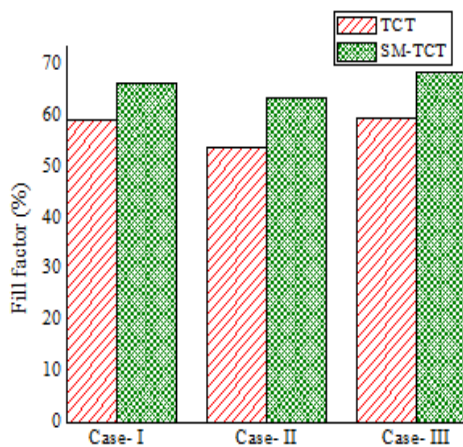**Fig. 9** PE of SM-TCT configuration for regular shading cases: I-III

Fig. 10 Fill factor of TCT and SM-TCT configurations for regular shading cases: I-III

4.5. Performance ratio

The PR is evaluated for considered shading cases: I-III. In the case of shading-I, the value of PR is enhanced from 0.781 to 0.875 for TCT and SM-TCT respectively. The assessed PR values are shown in Table 2 for both PV array settings and in Figure 11 as,
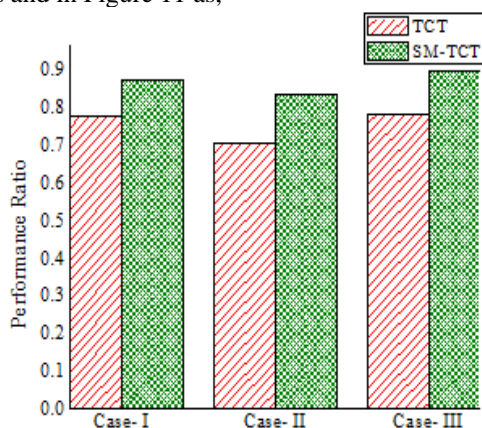

Fig. 11 PR of TCT and SM-TCT configurations under regular shading cases: I- III

6. Conclusion

In this paper, a research is conducted to perform the comparison of SM puzzles and contrasts the current TCT configuration for three distinct shading cases, such as minimal energy loss, worldwide output, and FF improvement. Extensive tests for different shading models, namely (i) lamp post shading (ii) Three cornered shading or structure shading (iii) Single vertex shading, are performed on these settings. The performance of these settings is contrasted with regard to shading patterns and the performance of the PV module configured by SM-TCT is noted to be better than the TCT setup. Overall, the research is helpful and will be a benchmark for scientists, business participants and engineering in this region.

Acknowledgements

References

[1] Goss, B., Cole, I., Betts, T., Gottschalg, R. (2014) Irradiance modelling for individual cells of shaded solar photovoltaic arrays. *Solar Energy* **110**: 410–419.

[2] Kumar, A., Pachauri, R. K., Chauhan, Y. K. (2016) Experimental analysis of SP / TCT PV array configurations under partial shading conditions. *Proc. Int. Conf. on Power Electr., Int. Cont. and Energy System.* 1–5.

[3] Yadav, A. S., Pachauri, R. K., Chauhan, Y. K. (2016) Comprehensive investigation of PV arrays with puzzle shade dispersion for improved performance. *Solar Energy* **129**: 256–285.

[4] Patel, H., Agarwal, V. (2008) Maximum power point tracking scheme for PV systems operating under partially shaded conditions. *IEEE Transactions on Industrial Electronics* **55(4)**: 1689 – 1698.

[5] Rani, B. I., Ilango, G. S., Nagamani, C. (2013) Enhanced power generation from PV array under partial shading conditions by shade dispersion using Su-Do-Ku configuration. *IEEE Trans. Sustain. Energy* **4(3)**: 594–601.

[6] Fialho, L., Melicio, R., Mendes, V. M. F., Figueiredo, J., Pereira, M. C. (2014) Effect of shading on series solar modules: simulation and experimental results. *Procedia Technology* **17**: 295–302.

[7] Koray, K. S. (2014). FPGA based new MPPT method for PV array system operating partially shaded conditions. *Energy* **68**: 399–410.

[8] Moballegh, S., Jiang, J., (2014) Modeling, prediction, and experimental validations of power peaks of PV arrays under partial shading conditions. *IEEE Trans. Sustain. Energy* **5(1)**: 293–300.

[9] Pareek, S., Dahiya, R. (2014) Output power maximization of partially shaded 4×4 PV field by altering its topology. *Energy Procedia* **54**: 116–126.

[10] Qi, J., Zhang, Y., Chen, Y. (2014) Modelling and maximum power point tracking (MPPT) method for PV array under partial shade conditions. *Renewable Energy* **66**: 337–345.

[11] Ramaprabha, R. (2014) Selection of an optimum configuration of solar PV array under partial shaded condition using particle swarm optimization. *Int. Journal of Elect., Comp., Energ., Electr. and Comm. Engineering* 8(1): 96–103.

[12] Vijayalekshmy, S., Iyer, S. R., Beevi, B. (2014). Comparative analysis on the performance of a short string of series connected and parallel connected photovoltaic array under partial shading. *J. Inst. Eng. India Ser. B,* **96(3)**: 217-226.

[13] Bai, J., Cao, Y., Hao, Y., Zhang, Z., Liu, S., Cao, F. (2015) Characteristic output of PV systems under partial shading or mismatch conditions. *Solar Energy* **112**: 41–54.

[14] Deshkar, S. N., Dhale, S. B., Mukherjee, J. S., Babu, T. S., Rajasekar, N. (2015) Solar PV array reconfiguration under partial shading conditions for maximum power extraction using genetic algorithm *Renew. Sustain. Energy Reviews* **43**: 102–110.

[15] Malathy, S. Ramaprabha, R. (2015) Comprehensive analysis on the role of array size and configuration on energy yield of photovoltaic systems under shaded conditions. *Renew. Sustain. Energy Reviews* **49**: 672–679.

[16] Rao, P. S., Dinesh, P., Ilango, G. S., Nagamani, C. (2015) Optimal Su-Do-Ku based interconnection scheme for increased power output from PV array under partial shading conditions. *Front. Energy* **9(2)**: 199–210.

[17] Vijayalekshmy, S., Bindu, G. R., Iyer, S.R. (2015) Analysis of various photovoltaic array configurations under shade dispersion by Su-Do-Ku arrangement during passing cloud conditions. *Indian J. Sci. Technology* **8(35)**: 2015.

[18] Vijayalekshmy, S., Bindu, G. R., Iyer, S. R. (2015) Performance improvement of partially shaded photovoltaic arrays under moving shadow conditions through shade dispersion. *J. Inst. Eng. Series- B*: 1–7.

[19] Yadav, A. S., Pachauri, R. K., Chauhan, Y. K. (2016) Comprehensive investigation of PV arrays under different shading patterns by shade dispersion using puzzled pattern based Su-Do-Ku puzzle configuration. *Proc. Int. Conf. Next Generation Computer Technology:* 824–830.

[20] Sahu, H. S., Nayak, S. K. (2016) Extraction of maximum power from a PV array under non-uniform irradiation conditions. *IEEE Trans. Electron Devices* **63(12)**: 4825–4831.

[21] Sahu, H. S., Nayak, S. K., Mishra, S. (2016) Maximizing the power generation of a partially shaded PV array. *IEEE J. Emerg. Sel. Top. Power Electron* **4(2)**: 626–637.

[22] Pareek, S., Chaturvedi, N., Dahiya, R. (2017) Optimal interconnections to address partial shading losses in solar photovoltaic arrays. *Solar Energy* **155**: 537–551.

[23] Pachauri, R., Singh, R., Gehlot, A., Samakaria, R., Choudhury, S. (2019). Experimental analysis to extract maximum power from PV array reconfiguration under partial shading conditions. Engineering Science and Technology, an International Journal 22: 109–130.

[24] Haq, A.U., Alammari, R., Iqbal, A., Jalal, M., Gul, S. (2020) Computation of power extraction from photovoltaic arrays under various fault conditions. IEEE Access 8: 47619-47639.